

Northeast Atlantic Storm Activity and Its Uncertainty from the Late Nineteenth to the Twenty-First Century

OLIVER KRUEGER, FRAUKE FESER, AND RALF WEISSE

Institute of Coastal Research, Helmholtz-Zentrum Geesthacht, Geesthacht, Germany

(Manuscript received 6 August 2018, in final form 16 January 2019)

ABSTRACT


Geostrophic wind speeds calculated from mean sea level pressure readings are used to derive time series of northeast Atlantic storminess. The technique of geostrophic wind speed triangles provides relatively homogeneous long-term storm activity data and is thus suited for statistical analyses. This study makes use of historical air pressure data available from the International Surface Pressure Databank (ISPD) complemented with data from the Danish and Norwegian Meteorological Institutes. For the first time, the time series of northeast Atlantic storminess is extended until the most recent year available, that is, 2016. A multidecadal increasing trend in storm activity starting in the mid-1960s and lasting until the 1990s, whose high storminess levels are comparable to those found in the late nineteenth century, initiated debate over whether this would already be a sign of climate change. This study confirms that long-term storminess levels have returned to average values in recent years and that the multidecadal increase is part of an extended interdecadal oscillation. In addition, new storm activity uncertainty estimates were developed and novel insights into the connection with the North Atlantic Oscillation (NAO) are provided.

1. Introduction

Long observational records of wind are rare and often inhomogeneous (e.g., Wan et al. 2010; Lindenberg et al. 2012), as such time series of wind speed observations can be affected by changes of the types of instruments used (including calibration and maintenance), by station relocations, and by physical changes in station surroundings (e.g., Schmith et al. 1997; Weisse et al. 2009; Feser et al. 2015). Consequently, direct wind measurements are a less effective measure for storminess and for the assessment of long-term storm activity. Furthermore, inhomogeneities potentially impair analyzed products, such as weather maps or long reanalyses, and hinder the evaluation of long-term trends of storm activity (Bengtsson et al. 2004; Ferguson and Villarini 2012; Krueger et al. 2013; Ferguson and Villarini 2014; Befort et al. 2016; Bloomfield et al. 2018). As a result, it is now common practice to make use of long time series of pressure measurements to derive proxies for storm activity. Even though air pressure, like every measured

variable, certainly suffers from inhomogeneities, it is in comparison with wind measurements more skillful in terms of homogeneity and can be considered to be a robust variable. Near-surface air pressure as a spatially large-scale variable is mostly insensitive to local conditions or small-scale disturbances, for instance due to station relocations (Weisse and von Storch 2009). Furthermore, the method of measuring the surface air pressure did not change for centuries when using traditional barometers. Air pressure has thus been measured consistently for long periods. In some cases, observations longer than 100 years are available, providing long and relatively homogeneous data sources that can be utilized to describe long-term variations in storm activity qualitatively. In contrast, there are less similar long and homogeneous time series of wind speed observations (e.g., Cusack 2013).

Besides numerous air pressure-based proxies that utilize pressure readings from single weather stations (e.g., Bärring and von Storch 2004; Bärring and Fortuniak 2009; Krueger and von Storch 2012; Pingree-Shippee et al. 2018), the calculation of seasonal and annual statistics of geostrophic wind speeds over triangles of mean sea level pressure measurements is an established tool to derive storm activity over wider areas on longer time scales (Schmidt and von Storch 1993; Schmith 1995;

 Denotes content that is immediately available upon publication as open access.

Corresponding author: Oliver Krueger, oliver.krueger@hzg.de

DOI: 10.1175/JCLI-D-18-0505.1

© 2019 American Meteorological Society. For information regarding reuse of this content and general copyright information, consult the [AMS Copyright Policy](https://www.ametsoc.org/PUBSReuseLicenses) (www.ametsoc.org/PUBSReuseLicenses).

Schmith et al. 1998; Alexandersson et al. 1998, 2000; Matulla et al. 2008; Wang et al. 2009, 2011; Krueger and von Storch 2011). Here, the geostrophic wind speed acts as a proxy for the wind speed close to the surface. Its skill in representing storminess is best over flat terrain and sea surfaces in the mid- and high latitudes, where the atmospheric circulation is mostly geostrophic, and ageostrophic disturbances are negligible (Krueger and von Storch 2011; Feser et al. 2015). Wang et al. (2009) found good agreement between the proxy and ERA-40 storminess. Later, Krueger and von Storch (2011) evaluated the informational content of the proxy in general and found it to be skillful in describing past storm activity.

Alexandersson et al. (1998, 2000) analyzed high annual percentiles of geostrophic wind speeds over the northeast Atlantic Ocean and the Baltic Sea from 1881 onward [published within the WASA Group (1998) and as a follow-up study]. They found that storm activity in the northeast Atlantic was at high levels in the late nineteenth century, which declined slowly afterward until the 1960s. In the following, storminess increased until the 1990s to high levels with an ensuing decrease afterward. The peak in storm activity levels in the 1990s is comparable to that of the late nineteenth century. The results of Alexandersson et al. (1998, 2000) were confirmed by several later studies, consecutively extending the time series of northeast Atlantic storminess until 2007 (e.g., Trenberth et al. 2007; Matulla et al. 2008; Wang et al. 2009, 2011, 2014).

Storm activity is influenced by the large-scale atmospheric variability, such as weather patterns and oscillations. The North Atlantic Oscillation (NAO), which is one such pattern, describes the pressure variability between the Icelandic low and the Azores high. The NAO is quantified through the NAO index, which is either based on standardized pressure differences between Iceland and the Azores (Hurrell 1995), or is based on pattern decomposition of Northern Hemisphere surface pressure or of geopotential height fields at different pressure levels (Barnston and Livezey 1987).

The NAO is the dominant mode of pressure variability over the North Atlantic and affects the generation of storms to a large extent (Wanner et al. 2001; Pinto and Raible 2012). During high values of the NAO index, often found in winter, pressure differences and the frequency of low-pressure systems increase. Associated frontal systems with temperature and pressure gradients may lead to increased storm genesis, increased zonal flow, and storm activity (Feser et al. 2015). For instance, Donat et al. (2010) found that the majority of storm events take place during periods with a positive value for the NAO index. Raible (2007), who analyzed ERA-40 data, found that midlatitude cyclones are linked

to the large-scale winter circulation. Raible (2007) relates the cyclone activity index with the 500-hPa geopotential height and obtains a correlation structure similar to the pattern of the NAO. Pinto et al. (2009) note that although a positive NAO index leads to more frequent and intense storms, severe storms can also occur during negative NAO phases.

Studies that focused on the evaluation of pressure-based proxies and examined the relationship between northeast Atlantic storminess and the NAO found differing results. Alexander et al. (2005) analyzed the frequency of strong pressure changes occurring in winter as a measure for storm activity and found high correlations with the NAO over the British Isles and Iceland. Hanna et al. (2008) investigated the relation of the NAO and storm frequencies over northern Europe and found a positive link, but noted that the link is weaker in southern parts of the domain. Allan et al. (2009) assessed storm activity over the British Isles from the 1920s onward and found the correlation with the NAO to be lower than that of the above-mentioned studies. Matulla et al. (2008), when assessing long storminess time series for the northeast Atlantic, write that “the NAO index is not helpful to describe storminess” (p. 130) as correlations are weak to medium (up to $r = 0.44$). Furthermore, they note that the link between storminess and the NAO is not stationary over time, which is also shown by Pinto and Raible (2012) and Raible et al. (2014).

This study assesses the annual time series of northeast Atlantic storminess based on high percentiles of geostrophic wind speeds in the period 1875–2016, including its connection to the NAO, and presents new uncertainty estimates derived through a bootstrapping approach. The manuscript is structured as follows: The second section describes the data being used and the derivation of the storminess time series including their uncertainty. Afterward, the third section presents and discusses obtained results, followed by the conclusions. The appendix provides more detailed information about the derivation of geostrophic wind speeds.

2. Data and methods

a. Preparation

In our analysis we make use of pressure data from the International Surface Pressure Databank (ISPD; Compo et al. 2015; Cram et al. 2015), which is a vast collection of historical surface pressure observations ordered in time and space with WMO station codes being used as identifiers. While the dataset as a whole currently ends in 2016, the time period covered differs among individual stations depending on the beginning and end of

TABLE 1. WMO number, country, name, coordinates, and observational period of the stations used. Numbers in parentheses denote alternate identifiers. For Denmark, alternate numbers denote national climate identifiers as an aggregation used for neighboring stations. For Bergen, the original station 01316 was replaced by station 01317, and missing values were filled with values from station 01311 positioned a few kilometers away.

Number	Country	Name	Latitude	Longitude	Period
01001	Norway	Jan Mayen	70.93°N	8.67°W	1922–2016
01152	Norway	Bodø	67.27°N	14.43°E	1900–2016
01316 (01317, 01311)	Norway	Bergen	60.38°N	5.33°E	1868–2016
03091	Great Britain	Aberdeen	57.2°N	2.2°W	1871–2016 (missing 1948–56)
03953	Ireland	Valentia	51.93°N	10.25°W	1892–2016
04013	Iceland	Stykkisholmur	65.08°N	22.73°W	1874–2016
06011	Faroe Islands	Torshavn	62.02°N	6.77°W	1874–2016
06260	Netherlands	de Bilt	52.1°N	5.18°E	1897–2016
06051 (21100)	Denmark	Vestervig	56.73°N	8.27°E	1874–2016
06088 (25140)	Denmark	Nordby	55.47°N	8.48°E	1874–2016

measurement activities. Furthermore, the ISPD provides metadata indicating the quality of measurements. These quality flags originate as feedback from creating the Twentieth Century Reanalysis (20CR; appendix B in Compo et al. 2011) and are available until 2013. Based on these metadata we excluded all the measurements for which the quality-control (QC) flags indicated poor data quality. 20CR uses an automatic quality control procedure, which might exclude extremely low surface pressure values. Pressure data of the years 2014–16, for which these metadata are not available, were screened for errors and partly evaluated by comparing with data available from the Norwegian Meteorological Institute (2018) and the Danish Meteorological Institute (Cappelen 2018a,b), which we also used as further validation of our own data mining routines.

The derivation of geostrophic wind speeds requires pressure observations at sea level. Our data, extracted from the ISPD, often consisted of pressure observations that were not reduced to the mean sea level. In those cases we applied a height reduction based on international standard atmospheric values, as we lack information about the state of the atmosphere at the time of pressure measurements, which would be needed to reduce the air pressure in a more sophisticated manner. Following Alexandersson et al. (1998), who used the barometric formula, the pressure reduction from height h to the mean sea level reads

$$p_0 = p(h) \left(1 + \frac{h}{T_0} \frac{\partial T}{\partial h} \right)^{-Mg/[R \times (\partial T/\partial h)]}, \quad (1)$$

where M is the molar mass of air ($0.02896 \text{ kg mol}^{-1}$), R is the gas constant ($8.314 \text{ J mol}^{-1} \text{ K}^{-1}$), and g is the gravitational acceleration (9.807 m s^{-2}). When assuming a temperature T_0 at sea level of 288.15 K , a lapse rate

$\partial T/\partial h$ of -0.0065 K m^{-1} (values for the U. S. standard atmosphere), Eq. (1) becomes

$$p_0 = p(h) \left(1 - \frac{0.0065 \text{ K m}^{-1} h}{288.15 \text{ K}} \right)^{-5.255}. \quad (2)$$

As a last preparatory step, the measurement data need to be simultaneous. In earlier times, measurements were taken at specific hours multiple times a day and were bound by local time zones. As a consequence, the available subdaily pressure data are misaligned in time, which we need to correct. We achieved the temporal synchronization through interpolating the pressure observations from one station in time via a cubic spline interpolation to 3-hourly values at 0000, 0300, 0600, 0900, 1200, 1500, 1800, and 2100 UTC. Here, we made use of the R-package zoo (Zeileis and Grothendieck 2005) and allowed for a maximum gap of 13 h between available time steps. Time steps for which the temporal interpolation is not possible are denoted as not available.

b. Northeast Atlantic storminess

In our approach, we aim at following Alexandersson et al. (1998, 2000) and make use of 10 stations (Table 1) forming 10 triangles of geostrophic wind speeds given in Fig. 1 and Table 2. The time series over some triangles extend back to years earlier than 1875. Pressure observations and geostrophic winds prior to 1875 are omitted, as uncertainties increase in historical times because of sparse data availability and insecurities related to the documentation of earlier pressure readings. The station Aberdeen does not provide observations during the period 1948–56, which affects five triangles in our analysis. Contrary to Wang et al. (2009), we do not replace the missing period by filling the gap with data from a different station relatively nearby, but address the issue through our uncertainty analysis.

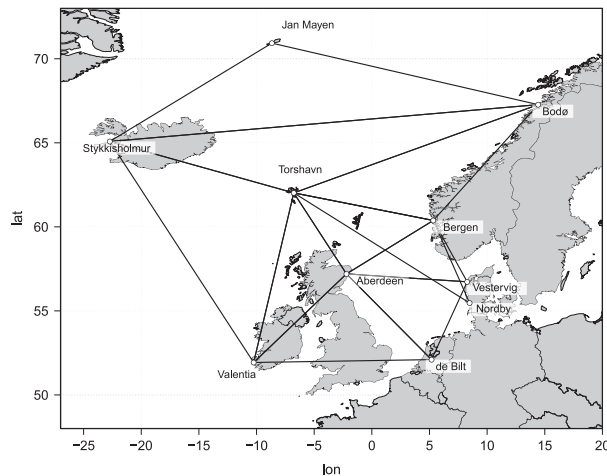


FIG. 1. Pressure observations from 10 stations have been used to derive geostrophic wind speeds from 10 triangles over the northeast Atlantic and European regions following Alexandersson et al. (2000).

For each of the triangles we calculate geostrophic wind speeds (the appendix provides a detailed description), from which we derive seasonal and annual frequency distributions. Those are then utilized to derive seasonal and annual 95th and 99th percentiles as a measure for moderate and extreme storm activity. Depending on the location of the triangle the magnitudes of the percentile time series differ substantially. To bring the percentile time series into the same range, the individual triangle time series of percentiles are standardized by subtracting the average and by dividing through the standard deviation of the triangle time series individually. We use averages and standard deviations of the period 1881–2010 (where available). The obtained time series are dimensionless but can be understood as the number of standard deviations away from the long-term average. The standardization does not change the underlying distribution of the considered quantiles as it only changes the range and units. However, there is no reason to assume that individual quantiles do not follow a normal distribution (Walker 1968). The standardized time series of the 10 triangles are then averaged separately for the 95th- and 99th-percentile time series to obtain one annual time series representative for seasonal or yearly northeast Atlantic storm activity. Note that unexpected differences between the averages of the standardized 95th and 99th percentiles are a possible result of the applied standardization procedure as the percentile time series are standardized individually (e.g., when the standardized and averaged 99th percentiles are smaller than the standardized and averaged 95th percentiles).

TABLE 2. Triangles and time periods used to construct mean values within the Northeast Atlantic.

Triangle	Time period
Torshavn–Stykkisholmur–Bodø	1900–2016
Bergen–Torshavn–Aberdeen	1875–2016 (missing 1948–56)
Torshavn–Bodø–Bergen	1900–2016
Aberdeen–Valentia–Torshavn	1892–2016 (missing 1948–56)
Bergen–Vestervig–Aberdeen	1875–2016 (missing 1948–56)
Aberdeen–Valentia–de Bilt	1902–2016 (missing 1948–56)
Aberdeen–Vestervig–de Bilt	1902–2016 (missing 1948–56)
Valentia–Stykkisholmur–Torshavn	1892–2016
Jan Mayen–Stykkisholmur–Bodø	1922–2016
Torshavn–Nordby–Bergen	1875–2016

c. Uncertainty

Even though pressure measurements are mostly homogeneous, pressure measurements, and consequently northeast Atlantic storminess time series, are still prone to uncertainties due to measurement routines, conversion, digitization, sampling errors (see Schmith et al. 1997; Alexandersson et al. 1998), data availability, and pre-processing of the data including temporal interpolation and height correction. So far, the reported storminess time series in the northeast Atlantic do not include estimates of uncertainty.

To overcome this lack of information, we applied a bootstrapping approach (Efron and Tibshirani 1986; DiCiccio and Efron 1996) instead of examining individual sources of uncertainty. We assume that the bootstrapping applied uncovers the uncertainty in storminess time series inherited from sampling and from uncertainties apparent in pressure observations. Bootstrapping describes a technique to estimate sample distributions of statistics nonparametrically through random sampling with replacement, which we apply in two steps to the time series of northeast Atlantic storm activity. First, we bootstrapped annual 95th and 99th percentiles of geostrophic wind speeds for each triangle and year separately. Through randomly selecting between 80% and 99.99% of the data available for each year and subsequently calculating 95th and 99th percentiles of geostrophic wind speeds, we build distributions thereof for each year and triangle separately consisting of 2500 samples of percentiles each. Second, from these annual distributions we draw yearly time series of annual percentiles for each triangle randomly, which are then standardized and averaged. By repeatedly applying this procedure, we obtain 100 000 realizations of the northeast Atlantic storminess time series, from which we calculate yearly 2.5th and 97.5th percentiles as the lower and upper bounds of a 95% confidence interval. Every value that falls within the 95% confidence interval does not differ significantly from the northeast Atlantic storminess time series derived after Alexandersson et al. (1998, 2000)

at the 0.05 significance level. Seasonal uncertainty is determined correspondingly.

We determined the value of 80% of annual and seasonal data availability as a lower limit through a sensitivity analysis, in which we examined systematically how data availability affects uncertainty estimates. As a result we found that the uncertainty remains almost stable for a data availability greater than 80%. Note that our approach also treats missing data equally, thereby automatically adjusting (inflating) the uncertainty in periods that have no data available.

3. Results and discussion

a. Storm activity

Figure 2 shows the time series of standardized and averaged annual 95th and 99th percentiles of geostrophic wind speeds over the northeast Atlantic for the period 1875–2016. The time series of annual percentiles show pronounced interannual and interdecadal variability. Interdecadal variability is highlighted by applying a Gaussian low-pass filter with $\sigma = 3$ denoting the standard deviation of the underlying Gaussian distribution of the low-pass filter. The annual time series indicate high storminess levels in the late nineteenth century (with maxima at 1.77 in 1877 for the 95th percentile and 1.63 in 1881 for the 99th percentile), from which storm activity declines to average levels in the turn of the centuries. Storminess rises again in the following years and decreases gradually to subaverage values in the 1930s, followed by an increase until around 1950. From 1950 to the 1960s, we see a sharp decline in storminess. The following decades indicate a remarkable upward trend in storminess from the calmer 1960s to the mid-1990s to storminess levels similar and slightly greater than those found in the late nineteenth century with maxima at 1.63 in 1990 for the 95th percentile and 1.98 in 1993 for the 99th percentile.

Storminess levels in the late 1990s and 2000s are characterized by a decrease in storminess to average or subaverage values in 2010. The reported annual values of storminess in 2010 of -1.8 and -1.7 (95th and 99th percentiles) denote the absolute minimum in storm activity over the examined period. The following years again show an increase in storminess. The magnitude of storminess depends on the regarded region and percentile, but corresponds to wind speeds of at least 7 on the Beaufort scale (Bft; 14.4 m s^{-1}) for the 95th percentile and at least 8 Bft (17.5 m s^{-1}) for the 99th percentile of geostrophic wind speed. For instance, 2009 and 2010 are the two years with the lowest values of storm activity. In these years, the triangle Jan Mayen–Stykkisholmur–Bodø shows 16.45 and 16.39 m s^{-1} (19.38 and 21.75 m s^{-1}) for the

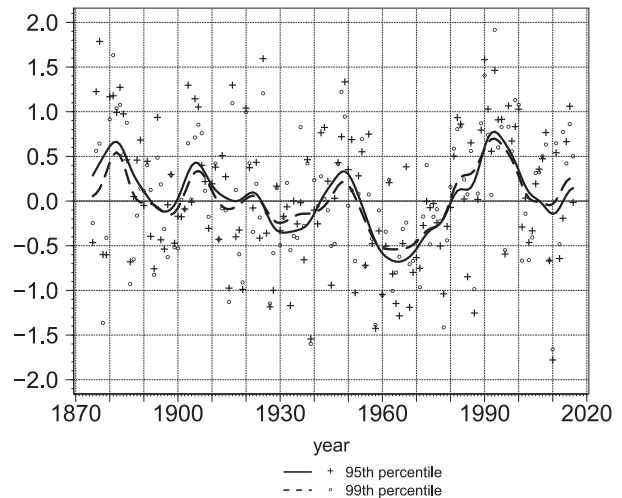


FIG. 2. Standardized time series of annual 95th (plus signs) and 99th (circles) percentiles of geostrophic wind speeds averaged over 10 triangles in the northeast Atlantic. Solid and dashed lines denote low-pass-filtered time series.

95th percentile (99th percentile) of geostrophic wind speed. Apart from these two years, all values obtained over the triangles are greater than 8 Bft. The results obtained confirm and extend previous results (Schmith et al. 1998; Alexandersson et al. 1998, 2000; Wang et al. 2009; Matulla et al. 2008) to 2016. Furthermore, our results are also backed independently by a study that homogenizes long wind speed measurements from the Netherlands to calculate storm loss indices (Cusack 2013). The temporal evolution of their presented time series of the 10-yearly number of damaging storms over the Netherlands is very similar to our low-pass-filtered annual time series seen in Fig. 2. Unfortunately, long and homogeneous wind speed time series as analyzed in Cusack (2013) are rarely found, making the use of pressure-based proxies for past storm activity inevitable.

Examining storminess time series on the seasonal scale helps to understand the annual time series in more detail. Therefore, the time series are standardized by using the annual long-term average and standard deviation instead of seasonal values to make the seasonal time series comparable to each other and to the annual time series. As a result, seasonal contributions to the overall annual time series become distinguishable. Storminess on the seasonal scale (Fig. 3) shares similarities and characteristics with that of annual high percentiles of geostrophic wind speeds, such as the pronounced interannual and interdecadal variability. However, there are notable differences in the behavior of the time series between individual seasons. First, as the seasonal time series shown in Fig. 3 are standardized

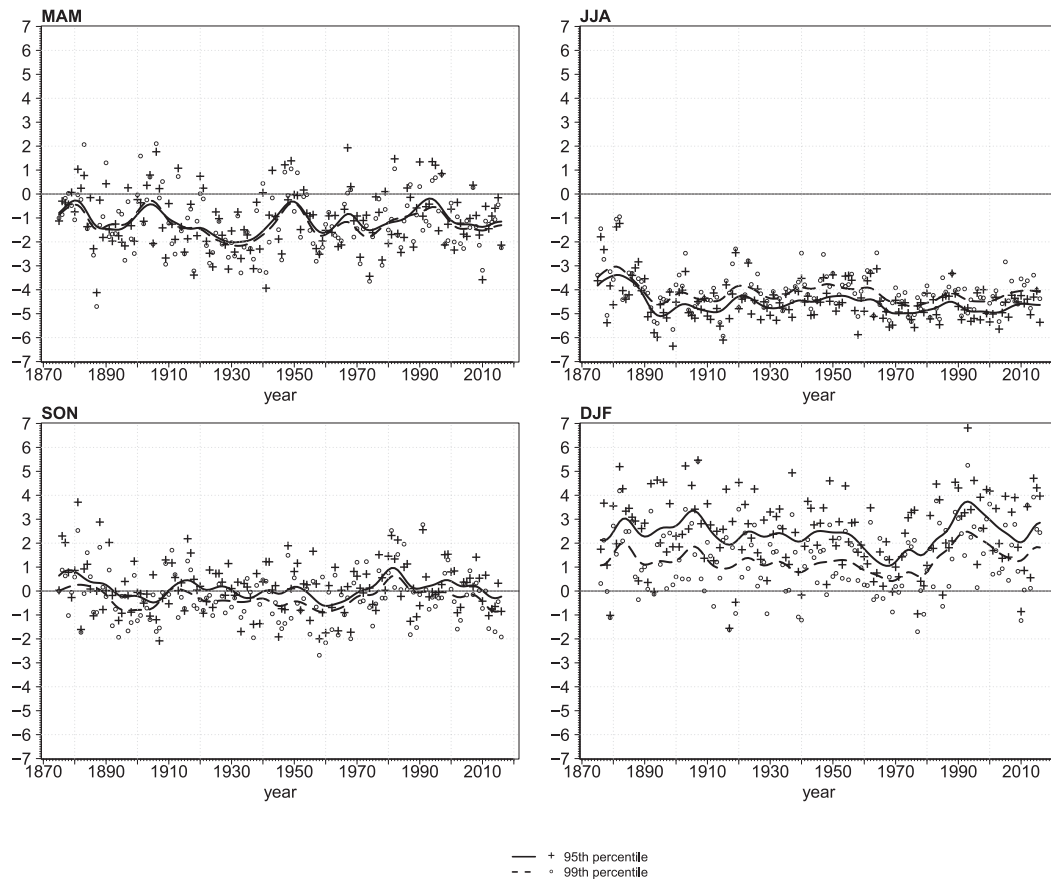


FIG. 3. Standardized time series of seasonal 95th and 99th percentiles of geostrophic wind speeds averaged over 10 triangles in the northeast Atlantic. Solid and dashed lines denote low-pass-filtered time series. Note that seasonal time series are standardized by the same annual time series used to standardize Fig. 2.

by the same annual time series used for Fig. 2, the figure reveals that the magnitude of storminess in the summer seasons is weaker than that of the other seasons to a great extent. Even the maximum of JJA storminess in the early 1880s is weaker than the long-term average of storm activity. Storm activity in spring is in general lower than the long-term average. SON storm activity oscillates around the long-term average of storm activity. Furthermore, as the figure shows, the magnitude of DJF storminess is the largest among the seasons indicating that the annual wind speed distribution is dominated by winter storm activity. Second, it is the interplay of storm activity during fall, winter, and spring that determines the overall storm climate in the northeast Atlantic as those storminess time series are very similar to that of annual northeast Atlantic storminess in their evolution. We also see that the low level of annual storminess in the 1960s starts with lower levels of storm activity in spring and fall, when winter storminess is still declining. Winter storminess declines further until

about 1970, when fall storminess is already on the rise again. Further, fall storminess finds its peak shortly after 1980 and declines to average values afterward, whereas winter storm activity rises until the beginning of the 1990s (topping storminess values around 1880 during winter 1991/92), declines until 2010, and increases afterward.

b. Storm activity and the North Atlantic Oscillation

Over the northeast Atlantic the atmospheric circulation is determined by the NAO to a great extent (Hurrell 1995). We explore the relationship of northeast Atlantic storminess with the NAO by comparing the time series of storminess with that of the similarly long NAO index time series based on the difference of normalized sea level pressure (SLP) between Lisbon, Portugal and Stykkisholmur/Reykjavik, Iceland since 1864 retrieved from NCAR (2018). For the analysis we use the seasonal and annual NAO index. The annual and low-pass-filtered time series of the NAO index are shown in Fig. 4 along with the low-pass-filtered time

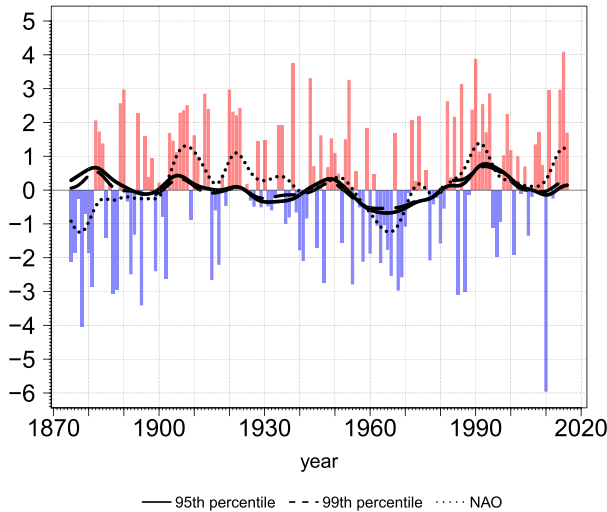


FIG. 4. Annual NAO index and low-pass-filtered time series of the NAO index 95th and 99th annual percentiles of geostrophic wind speeds averaged over 10 triangles in the northeast Atlantic.

series of northeast Atlantic storminess. The long-term variability of the NAO index, in particular of the low-pass-filtered time series, is quite similar to that of the storminess time series, but also shows some differences. In the beginning of the period analyzed, storminess is high, but the NAO is low, when we find relatively high values of summer storminess (see Fig. 3). Shortly afterward, high values can be found in the beginning of the twentieth century with a decrease until the 1960s, followed by a subsequent increase until the 1990s, when storm activity peaks. Afterward the NAO finds its absolute minimum over the period analyzed, namely, -5.96 in 2010, which also coincides with the year having the lowest value in storminess (cf. Fig. 2). The year 2010 is associated with high values of the Greenland blocking index (GBI; Hanna et al. 2015) that describes the large-scale presence and strength of high pressure systems over Greenland. In winter 2010, which was one of the years with lowest values of geostrophic wind speed percentiles for the northernmost triangle, such a high pressure system expands from Greenland to Russia bringing the northeast Atlantic area under the influence of cold and calmer conditions than usual (Hanna et al. 2018). In the years thereafter, the NAO is mostly positive.

The relationship is further investigated through a correlation analysis between the (unfiltered) seasonal and annual NAO index and our storminess time series (Table 3). The highest correlations can be found for the winter season, for which the correlation ranges between

TABLE 3. Simultaneous correlation between the NAO index and northeast Atlantic storm activity time series for annual and seasonal scales for the period 1875–2016. Boldface values denote correlations significantly greater than 0 at a significance level of 0.01.

Correlation	MAM	JJA	SON	DJF	Annual
95th percentiles	0.3814	0.2077	0.1210	0.6882	0.5191
99th percentiles	0.2294	0.2046	0.0548	0.6250	0.4388

0.6250 (99th percentile) and 0.6882 (95th percentile). The correlation on the annual time scale is in a similar order with values from 0.4388 (99th percentile) to 0.5191 (95th percentile). We find that correlations in fall seasons are lowest without showing correlations significantly greater than 0 at the 0.01 level. Significance is determined through applying a Fisher transformation (Fisher 1915) of the correlation and testing whether the transformed values are significantly greater than 0. Earlier studies, such as Alexandersson et al. (1998) and Matulla et al. (2008), find similar values for the correlation.

As the link between the NAO and northeastern Atlantic storm activity is not constant over time (Matulla et al. 2008; Hanna et al. 2008; Pinto and Raible 2012), we calculated the correlation between annual time series over a moving window of a 31-yr time span (Fig. 5). We see that the correlations are positive for the whole period. The time series of correlations are weak in the

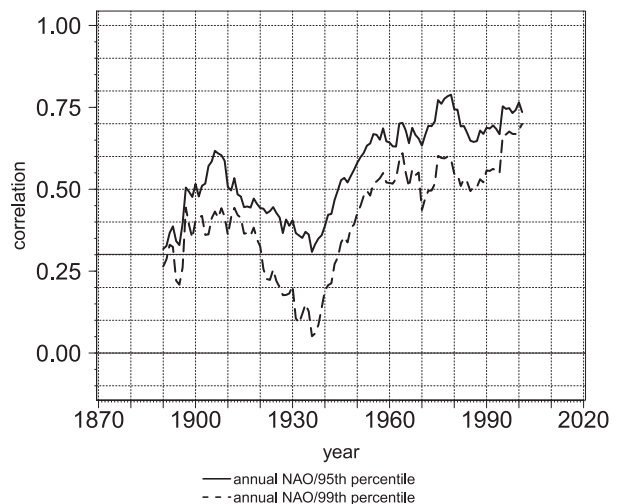


FIG. 5. Running correlation between the annual NAO index and the 95th and 99th annual percentiles of geostrophic wind speeds averaged over 10 triangles in the northeast Atlantic. The correlation has been calculated over a moving window of a 31-yr time span. Correlations shown represent correlations for the 15 years prior to and after a particular year. The horizontal solid line at 0.3012 denotes the critical value for a correlation significantly greater than 0 at the 0.05 level.

beginning and increase until 1905 to 0.6 (0.4) for the correlation with the annual 95th (99th) percentile. After a gradual decline, the period of the 1930s shows the weakest correlations, namely, 0.3 (95th percentile) and 0.05 (99th percentile). Afterward, the correlation increases steadily until the mid-1970s with maximum correlations found at 0.8 (95th percentiles) and 0.6 (99th percentiles), respectively. Whereas the correlation for the 95th percentile slightly declines and increases again to 0.75, the correlation for the 99th percentile rises to its maximum value, 0.7, at the end of the period. The correlation and its variability indicate the strength of the link between the North Atlantic Oscillation and northeast Atlantic storm activity and identify periods characterized by a weak connection. The period with the lowest correlations found is also the period when the 99th percentile is not significantly positively correlated with the NAO index at the 0.05 level, as the critical value for the correlation to be exceeded is 0.3012. In fact, while the 95th percentile is always significantly correlated, the 99th percentile is not during 1920–45.

Raible et al. (2014) found a similar relationship of the NAO dipole pattern over time derived from teleconnectivity maps of detrended winter 500-hPa geopotential height fields in 20CR calculated over moving windows spanning 30 years each. When comparing the most recent pattern with earlier patterns over the North Atlantic in the reanalysis, they found 1940–69 to be the period with the lowest agreement, showing an NAO dipole structure shifted to the west with a wave train-like pattern visible, which connects Greenland, the British Isles, and the eastern Mediterranean. Peings and Magnusdottir (2014) confirm this pattern in their analyses independently in the sea level pressure. Before and after that period, the strength of the link increases with maximum values found in recent times. Even though Raible et al. (2014) concentrate on teleconnection patterns at the 500-hPa geopotential height only (hence the shifted period), their analyses help explain our results, as in periods with low correlations between the NAO and northeast (NE) Atlantic storminess, other modes of atmospheric variability dominate. When these other modes are present and the NAO dipole pattern is shifted, the ability of the traditional station-based NAO index to describe the strength of the actual NAO and storminess diminishes. The station-based NAO index only represents atmospheric movements if the centers of the Azores high and Icelandic low pressure system as the poles of the North Atlantic Oscillation are near the stations used for deriving the NAO index. Possible changes in the NAO poles' location thus affect our correlation

analysis. Moreover, it is also possible to observe storm activity during NAO phases that are usually not associated with high levels of storm activity (Pinto et al. 2009), for example, in the 1880s. The atmospheric circulation structure and storm tracks may be shifted in such cases compared to a regular NAO structure, but storm activity would still be detectable by our method that covers a large spatial scale in the northeast Atlantic.

c. Uncertainty

Even though the time series of northeast Atlantic storminess after Alexandersson et al. (1998) is regarded as one of the most robust methods to derive long-term storm activity, it is still susceptible to inherent uncertainty, which results from uncertainties related to the air pressure observations, sampling and data availability, and processing of the data including our temporal interpolation and height correction. Our analysis therefore uses a bootstrapping approach to obtain information about the uncertainty of northeast Atlantic storminess. Figure 6 shows the time series of storm activity, including the 95% confidence interval. In addition, Fig. 7 depicts the range of the 95% confidence interval, and Fig. 8 depicts the same uncertainty range for each season. First, it is apparent that the uncertainty is higher for the time series based on 99th percentiles than for that of 95th percentiles. While the former ranges between 0.35 and 1.1, the latter only ranges between 0.3 and 0.8. Low-pass-filtered time series show a steadier 95% confidence interval, for which the values range between 0.5 and 1.0 (99th percentiles) and between 0.35 and 0.7 (95th percentiles). The differences between the uncertainties of the 95th and 99th percentiles result from sampling and consequently from the higher variability of the 99th percentiles compared to the 95th percentiles, as the sample size required to calculate the percentiles is higher for the upper percentile.

Second, uncertainty is highest in the early years as the time series of pressure observations was recorded less frequently back then and is prone to errors often resulting in data that have been removed during our data retrieval because of poor-quality flags. The two highest values of uncertainty in the early years, for instance, are 0.78 (1.1) and 0.84 (1.0) for the 95th (99th) annual percentiles in the years 1876 (1875) and 1889 (1880). After 1885, the uncertainty declines to about 0.4 (0.5) for the 95th (99th) percentiles and does not vary much from 1905 onward. This decline coincides with the addition of several triangles in 1892, 1900, 1902, and 1922 to the calculation, making the resulting storminess time series more robust. The

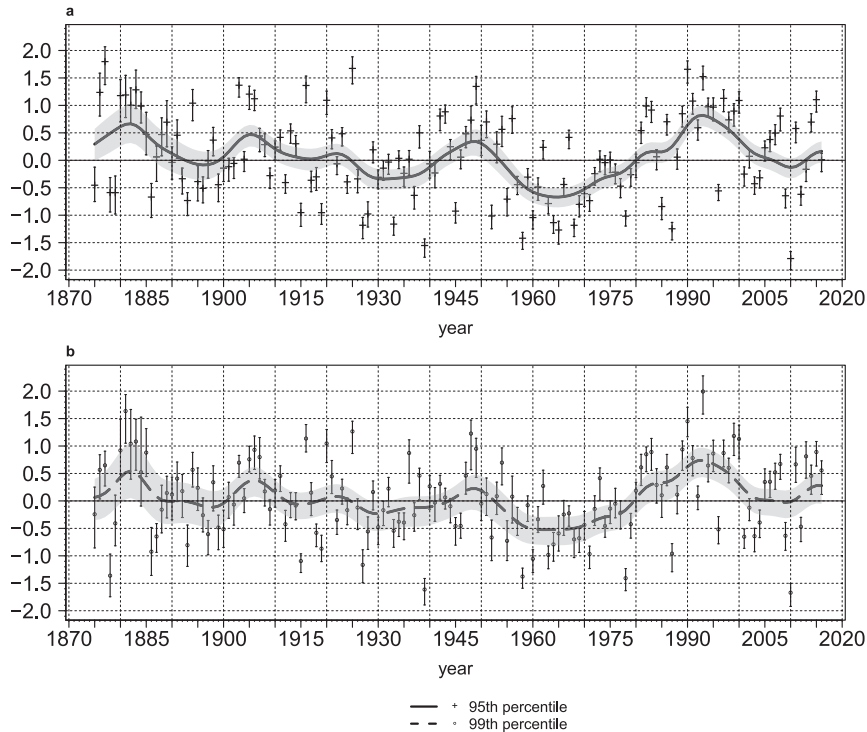


FIG. 6. Uncertainty estimates for northeast Atlantic storminess time series based on annual (a) 95th and (b) 99th percentiles of geostrophic wind speed. Shown are the annual values of storminess, including error bars denoting the 95% confidence interval. Lines indicate Gaussian low-pass-filtered time series including a 95% confidence interval.

missing years of the Aberdeen record during the period 1948–56, which affect the calculation of five triangles, are visible by an increase of the uncertainty up to 0.65 (0.9) for the 95th (99th) percentiles. The uncertainty of the low-pass-filtered time series rises to 0.5 and 0.67 for the 95th and 99th percentiles, respectively. After 1960, the uncertainty returns to previous levels but is slightly lower than before, likely because of better observation techniques. Compared with the early uncertainty, recent uncertainty is about half as high indicating a stronger representativity of storminess in more recent years. We noticed that since the second half of the twentieth century, air pressure is often recorded hourly, so that there is no need for interpolation.

Furthermore, Fig. 6, in particular Fig. 6b, illustrates that the uncertainty intervals are not centered symmetrically around storminess values derived from the full set of observed pressure data. As the bootstrapping applied does not presume any underlying distribution for storminess values, but samples from a thinned number of observed pressure data, the confidence interval provides the range of possible realizations, including the observed value for storminess.

Such a behavior does not necessarily mean that specific storminess quantiles are not normally distributed, but it does suggest that the true value for storminess might be shifted. From the same figure, we also see that even though storminess levels from observed pressure data are slightly higher in the early 1990s than those found in the late nineteenth century, the 95% confidence intervals overlap. Such an overlap suggests that storminess levels would not be statistically different from each other, which we are able to confirm at the 0.05 significance level when testing whether the differences between the observed values are significantly different from 0 (not shown).

The variability of the uncertainty on the seasonal scale is similar (Fig. 8) with notable differences. The seasonal uncertainty is higher than the annual uncertainty. Here, a decreased seasonal sample size leads to an amplification of the uncertainty, in particular in the years for which the data availability is low per se (i.e., low number of stations with a high number of missing or erroneous observations). For instance, the uncertainty in the earlier years reaches values of up to 2.3 for the seasonal 99th-percentile time series (e.g., in JJA 1881), while the maximum value of the annual

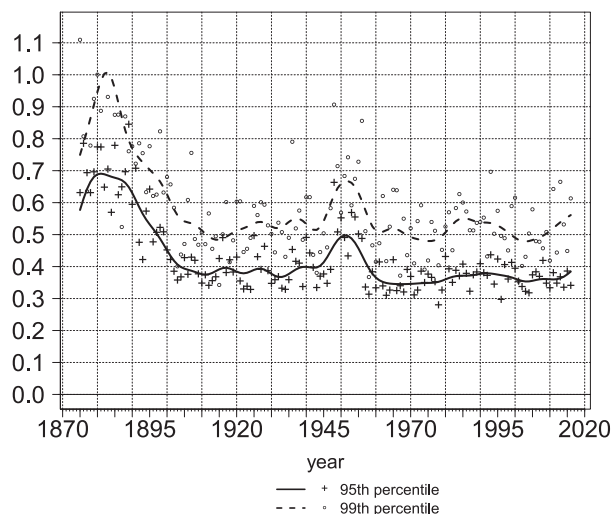


FIG. 7. Yearly values of uncertainty estimates for northeast Atlantic storminess time series based on annual 95th and 99th percentiles of geostrophic wind speed. Shown are the annual values of uncertainties as the range of the 95% confidence interval. Lines indicate the uncertainty of Gaussian low-pass-filtered time series as the range of the 95% confidence interval.

time series is 1.1. When all the stations are available and the overall data availability is high (later years), the seasonal uncertainty is in the range of 0.5–0.7 (0.8–1.0) for the 95th (99th) low-pass-filtered seasonal percentile time series and slightly higher for the unfiltered time series. The increase of uncertainty from annual to seasonal time scales indicates almost a doubling of uncertainty in storminess time series and puts less confidence in the estimates of seasonal storm activity in general, especially in the earlier years of the analyzed period.

When translating these uncertainty estimates from standardized values to physical units we make use of the derived values for the uncertainty and combine them with the standard deviations of the triangles. Using, for instance, a standard deviation of 1.10 m s^{-1} , which is the standard deviation of the annual 95th percentiles of storminess over the northernmost triangle (Jan Mayen–Stykkisholmur–Bodø), an annual uncertainty of about 0.5 standard deviations (at 1940) translates to an annual 95% confidence range of 0.55 m s^{-1} . For the Torshavn–Aberdeen–Bergen triangle, corresponding values would be 1.3 m s^{-1} (standard deviation) and 0.65 m s^{-1} (uncertainty range). On the seasonal scale, these values would be about twice as high. Alexandersson et al. (1998) suggested that errors in the pressure observations, time interpolation, and sampling can result in errors of $2\text{--}5 \text{ m s}^{-1}$ for the upper percentiles. Compared to their estimates, our uncertainty is an order of magnitude smaller. Even

though our bootstrapping approach assumes that at maximum 20% of the data is missing and, on top of that, also considers missing data, the estimate of Alexandersson et al. (1998) is more conservative and based on ad hoc parametric estimates. In comparison, our analysis uses nonparametric means to robustly approximate the time-varying uncertainty of northeast Atlantic storminess. Which uncertainty estimate proves to be more valid is not overly important, as there is only one realization of storm activity, but it provides valuable information about the representativity of storminess values over time.

4. Concluding remarks

Earlier studies focusing on shorter reanalyses or other numerical products report increases in storminess in the Atlantic sector [for an overview, see Feser et al. (2015) and Hartmann et al. (2013)] due to a relatively short time period. This initiated discussions about the potential impact of climate change on storminess. However, our long time series of northeast Atlantic storm activity helps to put the period from the 1960s to the 1990s, with its remarkable increase in storm activity, into a long-term perspective, with storminess revealing multidecadal variability.

The link with the NAO is found to be medium to good for the whole period analyzed, but it is weakest in the 1930s, indicating that other modes of atmospheric variability are present. After the 1930s, the link increases steadily to a stable connection that is characterized by a high correlation.

The newly developed uncertainty estimates are highest in the early years and for the period 1948–56, for which there are no observations at the Aberdeen station available. Data quality and availability directly affect the uncertainty estimates resulting in a reduced uncertainty in periods with high-quality data. Seasonal uncertainty is about twice as high as that of the annual time series, as the decreased seasonal sample size amplifies the uncertainty.

The increase from the 1960s to the 1990s and the following atmospheric stilling in northeast Atlantic storminess may already be a sign of changes expected as a result of climate change (Hartmann et al. 2013; Chang 2018; Barcikowska et al. 2018), which would agree with an eastward shift of the NAO centers of actions (Ulbrich and Christoph 1999). However, as recent studies highlight, the atmospheric circulation in the midlatitudes is dominated by internal variability (Raible et al. 2014; Hanna et al. 2018), making reliable projections about the future state of the circulation currently infeasible.

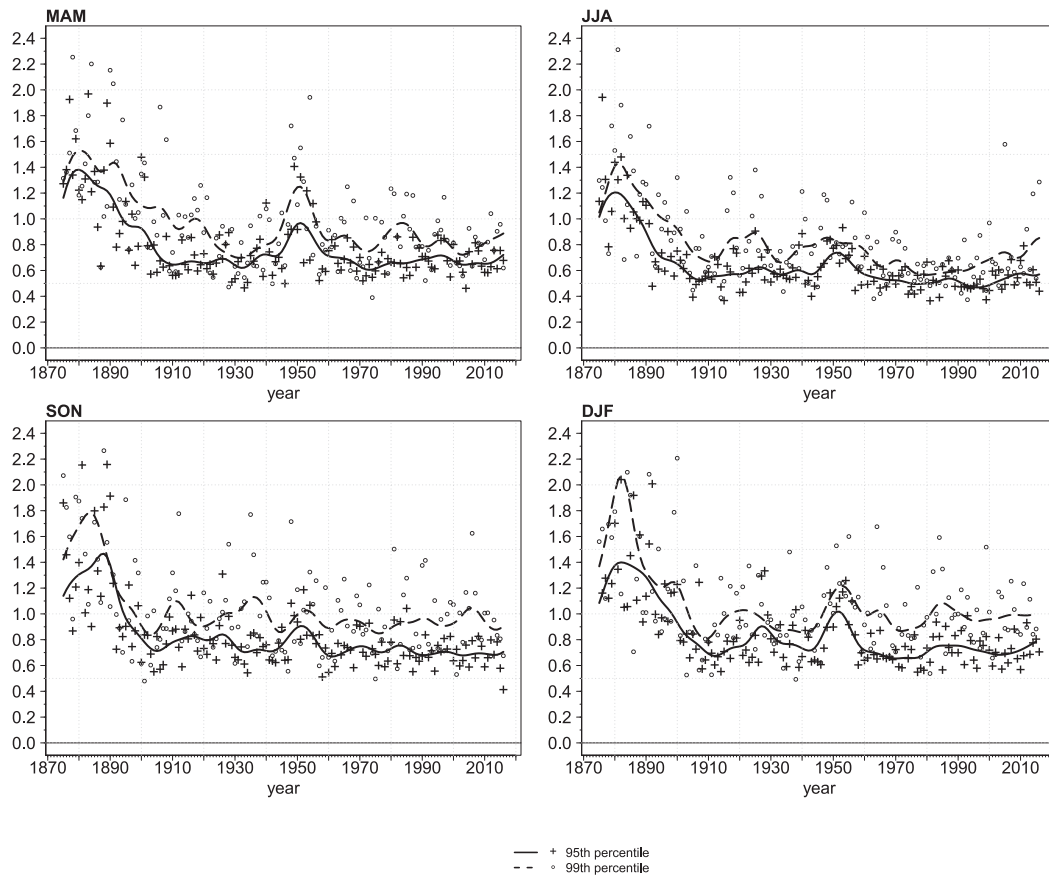


FIG. 8. Seasonal values of uncertainty estimates for northeast Atlantic storminess time series based on annual 95th and 99th percentiles of geostrophic wind speed. Shown are the seasonal values of uncertainties as the range of the 95% confidence interval. Lines indicate the uncertainty of Gaussian low-pass-filtered time series as the range of the 95% confidence interval.

Acknowledgments. The authors are grateful to Dr. Gil Compo, Chesley McColl, and Dr. Thomas Cram for providing air pressure data of the latest years. Further, the authors thank the ISPD and the Research Data Archive at the National Center for Atmospheric Research in Boulder, Colorado. They are also thankful to the Danish Meteorological Service and the Norwegian Meteorological Service for providing complementing data. This work is partially funded by the Bundesamt für Seeschifffahrt und Hydrographie BSH (German Federal Maritime and Hydrographic Agency). Moreover, the authors thank the anonymous reviewers in providing valuable suggestions.

APPENDIX

Derivation of Geostrophic Storminess

The approach of using geostrophic wind speeds to infer about the long-term climate of storminess, first

utilized by Schmidt and von Storch (1993), makes use of (simultaneous) triplets of pressure readings. The method, described in detail in Alexandersson et al. (1998), interpolates the mean sea level pressure observations $p_1, p_2,$ and p_3 over the area of the triangle determined through the set of station coordinates $(x_1, y_1), (x_2, y_2),$ and (x_3, y_3) . At each location (x, y) within the triangle, the pressure p is described as

$$p = ax + by + c. \tag{A1}$$

The coordinates x and y are given by

$$x = R_e \lambda \cos(\phi), \tag{A2}$$

$$y = R_e \phi, \tag{A3}$$

where R_e denotes Earth’s radius, λ denotes the longitude, and ϕ denotes the latitude. The coefficients $a, b,$ and c in Eq. (A1) can be derived by solving the following set of equations:

$$\begin{aligned} p_1 &= ax_1 + by_1 + c, \\ p_2 &= ax_2 + by_2 + c, \\ p_3 &= ax_3 + by_3 + c. \end{aligned} \quad (\text{A4})$$

The geostrophic wind speed is then calculated as

$$U_{\text{geo}} = (u_g^2 + v_g^2)^{1/2}, \quad (\text{A5})$$

with

$$u_g = -\frac{1}{\rho f} \frac{\partial p}{\partial y} = -\frac{b}{\rho f} \quad \text{and} \quad v_g = \frac{1}{\rho f} \frac{\partial p}{\partial x} = \frac{a}{\rho f}, \quad (\text{A6})$$

where ρ is the density of air (set at 1.25 kg m^{-3}) and f is the Coriolis parameter, which is usually the average of the Coriolis parameter at each measurement site. The coefficients a and b denote the zonal and meridional pressure gradients. After having derived U_{geo} at each time step, time series of geostrophic wind speed statistics can be obtained.

REFERENCES

- Alexander, L. V., S. F. B. Tett, and T. Jonsson, 2005: Recent observed changes in severe storms over the United Kingdom and Iceland. *Geophys. Res. Lett.*, **32**, L13704, <https://doi.org/10.1029/2005GL022371>.
- Alexandersson, H., T. Schmith, K. Iden, and H. Tuomenvirta, 1998: Long-term variations of the storm climate over NW Europe. *Global Atmos. Ocean Syst.*, **6**, 97–120.
- , H. Tuomenvirta, T. Schmith, and K. Iden, 2000: Trends of storms in NW Europe derived from an updated pressure data set. *Climate Res.*, **14**, 71–73, <https://doi.org/10.3354/cr014071>.
- Allan, R., S. Tett, and L. Alexander, 2009: Fluctuations in autumn–winter severe storms over the British Isles: 1920 to present. *Int. J. Climatol.*, **29**, 357–371, <https://doi.org/10.1002/joc.1765>.
- Barcikowska, M. J., S. J. Weaver, F. Feser, S. Russo, F. Schenk, D. A. Stone, M. F. Wehner, and M. Zahn, 2018: Euro-Atlantic winter storminess and precipitation extremes under 1.5°C vs. 2°C warming scenarios. *Earth Syst. Dyn.*, **9**, 679–699, <https://doi.org/10.5194/esd-9-679-2018>.
- Barnston, A. G., and R. E. Livezey, 1987: Classification, seasonality and persistence of low-frequency atmospheric circulation patterns. *Mon. Wea. Rev.*, **115**, 1083–1126, [https://doi.org/10.1175/1520-0493\(1987\)115<1083:CSAPOL>2.0.CO;2](https://doi.org/10.1175/1520-0493(1987)115<1083:CSAPOL>2.0.CO;2).
- Björing, L., and H. von Storch, 2004: Scandinavian storminess since about 1800. *Geophys. Res. Lett.*, **31**, L20202, <https://doi.org/10.1029/2004GL020441>.
- , and K. Fortuniak, 2009: Multi-indices analysis of southern Scandinavian storminess 1780–2005 and links to interdecadal variations in the NW Europe–North Sea region. *Int. J. Climatol.*, **29**, 373–384, <https://doi.org/10.1002/joc.1842>.
- Beftor, D. J., S. Wild, T. Kruschke, U. Ulbrich, and G. C. Leckebusch, 2016: Different long-term trends of extra-tropical cyclones and windstorms in ERA-20C and NOAA-20CR reanalyses. *Atmos. Sci. Lett.*, **17**, 586–595, <https://doi.org/10.1002/asl.694>.
- Bengtsson, L., S. Hagemann, and K. I. Hodges, 2004: Can climate trends be calculated from reanalysis data. *J. Geophys. Res.*, **109**, D11111, <https://doi.org/10.1029/2004JD004536>.
- Bloomfield, H. C., L. C. Shaffrey, K. I. Hodges, and P. L. Vidale, 2018: A critical assessment of the long-term changes in the wintertime surface Arctic Oscillation and Northern Hemisphere storminess in the ERA20C reanalysis. *Environ. Res. Lett.*, **13**, 094004, <https://doi.org/10.1088/1748-9326/aa5c5c>.
- Cappelen, J., Ed., 2018a: Denmark—DMI historical climate data collection 1768–2017. DMI Rep. 18–02, 111 pp., https://www.dmi.dk/fileadmin/user_upload/Rapporter/TR/2018/DMIRep18-02.pdf.
- , 2018b: The Faroe Islands—DMI historical climate data collection 1873–2017. DMI Rep. 18–05, 38 pp., https://www.dmi.dk/fileadmin/user_upload/Rapporter/TR/2018/DMIRep18-05.pdf.
- Chang, E. K.-M., 2018: CMIP5 projected change in Northern Hemisphere winter cyclones with associated extreme winds. *J. Climate*, **31**, 6527–6542, <https://doi.org/10.1175/JCLI-D-17-0899.1>.
- Compo, G. P., and Coauthors, 2011: The Twentieth Century Reanalysis project. *Quart. J. Roy. Meteor. Soc.*, **137**, 1–28, <https://doi.org/10.1002/qj.776>.
- , and Coauthors, 2015: The International Surface Pressure Databank version 3. Research Data Archive at the National Center for Atmospheric Research, Computational and Information Systems Laboratory, accessed 5 May 2018, <https://doi.org/10.5065/D6D50K29>.
- Cram, T. A., and Coauthors, 2015: The International Surface Pressure Databank version 2. *Geosci. Data J.*, **2**, 31–46, <https://doi.org/10.1002/gdj3.25>.
- Cusack, S., 2013: A 101 year record of windstorms in the Netherlands. *Climatic Change*, **116**, 693–704, <https://doi.org/10.1007/s10584-012-0527-0>.
- DiCiccio, T. J., and B. Efron, 1996: Bootstrap confidence intervals. *Stat. Sci.*, **11**, 189–228.
- Donat, M. G., G. C. Leckebusch, J. G. Pinto, and U. Ulbrich, 2010: Examination of wind storms over central Europe with respect to circulation weather types and NAO phases. *Int. J. Climatol.*, **30**, 1289–1300, <https://doi.org/10.1002/joc.1982>.
- Efron, B., and R. Tibshirani, 1986: Bootstrap methods for standard errors, confidence intervals, and other measures of statistical accuracy. *Stat. Sci.*, **1**, 54–75, <https://doi.org/10.1214/ss/1177013815>.
- Ferguson, C. R., and G. Villarini, 2012: Detecting inhomogeneities in the Twentieth Century Reanalysis over the central United States. *J. Geophys. Res.*, **117**, D05123, <https://doi.org/10.1029/2011JD016988>.
- , and —, 2014: An evaluation of the statistical homogeneity of the Twentieth Century Reanalysis. *Climate Dyn.*, **42**, 2841–2866, <https://doi.org/10.1007/s00382-013-1996-1>.
- Feser, F., M. Barcikowska, O. Krueger, F. Schenk, R. Weisse, and L. Xia, 2015: Storminess over the North Atlantic and north-western Europe—A review. *Quart. J. Roy. Meteor. Soc.*, **141**, 350–382, <https://doi.org/10.1002/qj.2364>.
- Fisher, R. A., 1915: Frequency distribution of the values of the correlation coefficient in samples from an indefinitely large population. *Biometrika*, **10**, 507–521, <https://doi.org/10.2307/2331838>.
- Hanna, E., J. Cappelen, R. Allan, T. Jónsson, F. Le Blancq, T. Lillington, and K. Hickey, 2008: New insights into North European and North Atlantic surface pressure variability, storminess, and related climatic change since 1830. *J. Climate*, **21**, 6739–6766, <https://doi.org/10.1175/2008JCLI2296.1>.
- , T. E. Cropper, P. D. Jones, A. A. Scaife, and R. Allan, 2015: Recent seasonal asymmetric changes in the NAO (a marked summer decline and increased winter variability) and associated changes in the AO and Greenland blocking index. *Int. J. Climatol.*, **35**, 2540–2554, <https://doi.org/10.1002/joc.4157>.

- , R. J. Hall, T. E. Cropper, T. J. Ballinger, L. Wake, T. Mote, and J. Cappelen, 2018: Greenland blocking index daily series 1851–2015: Analysis of changes in extremes and links with North Atlantic and UK climate variability and change. *Int. J. Climatol.*, **38**, 3546–3564, <https://doi.org/10.1002/joc.5516>.
- Hartmann, D. L., and Coauthors, 2013: Observations: Atmosphere and surface. *Climate Change 2013: The Physical Science Basis*, T. F. Stocker et al., Eds., Cambridge University Press, 159–254.
- Hurrell, J. W., 1995: Decadal trends in the North Atlantic Oscillation: Regional temperatures and precipitation. *Science*, **269**, 676–679, <https://doi.org/10.1126/science.269.5224.676>.
- Krueger, O., and H. von Storch, 2011: Evaluation of an air pressure–based proxy for storm activity. *J. Climate*, **24**, 2612–2619, <https://doi.org/10.1175/2011JCLI3913.1>.
- , and —, 2012: The informational value of pressure-based single-station proxies for storm activity. *J. Atmos. Oceanic Technol.*, **29**, 569–580, <https://doi.org/10.1175/JTECH-D-11-00163.1>.
- , F. Schenk, F. Feser, and R. Weisse, 2013: Inconsistencies between long-term trends in storminess derived from the 20CR reanalysis and observations. *J. Climate*, **26**, 868–874, <https://doi.org/10.1175/JCLI-D-12-00309.1>.
- Lindenberg, J., H. T. Mengelkamp, and G. Rosenhagen, 2012: Representativity of near surface wind measurements from coastal stations at the German Bight. *Meteor. Z.*, **21**, 99–106, <https://doi.org/10.1127/0941-2948/2012/0131>.
- Matulla, C., W. Schöner, H. Alexandersson, H. von Storch, and X. L. Wang, 2008: European storminess: Late nineteenth century to present. *Climate Dyn.*, **31**, 125–130, <https://doi.org/10.1007/s00382-007-0333-y>.
- NCAR, 2018: The climate data guide: Hurrell North Atlantic Oscillation (NAO) index (station-based). Accessed 11 July 2018, <https://climatedataguide.ucar.edu/climate-data/hurrell-north-atlantic-oscillation-nao-index-station-based>.
- Norwegian Meteorological Institute, 2018: eKlima.met.no: Climate and weather data. Accessed 1 June 2018, <http://eklima.met.no>.
- Peings, Y., and G. Magnusdottir, 2014: Forcing of the wintertime atmospheric circulation by the multidecadal fluctuations of the North Atlantic Ocean. *Environ. Res. Lett.*, **9**, 034018, <https://doi.org/10.1088/1748-9326/9/3/034018>.
- Pingree-Shippee, K. A., F. W. Zwiers, and D. E. Atkinson, 2018: Representation of mid-latitude North American coastal storm activity by six global reanalyses. *Int. J. Climatol.*, **38**, 1041–1059, <https://doi.org/10.1002/joc.5235>.
- Pinto, J. G., and C. C. Raible, 2012: Past and recent changes in the North Atlantic Oscillation. *Wiley Interdiscip. Rev.: Climate Change*, **3**, 79–90, <https://doi.org/10.1002/wcc.150>.
- , S. Zacharias, A. H. Fink, G. C. Leckebusch, and U. Ulbrich, 2009: Factors contributing to the development of extreme North Atlantic cyclones and their relationship with the NAO. *Climate Dyn.*, **32**, 711–737, <https://doi.org/10.1007/s00382-008-0396-4>.
- Raible, C. C., 2007: On the relation between extremes of midlatitude cyclones and the atmospheric circulation using ERA40. *Geophys. Res. Lett.*, **34**, L07703, <https://doi.org/10.1029/2006GL029084>.
- , F. Lehner, J. F. González-Rouco, and L. Fernández-Donado, 2014: Changing correlation structures of the Northern Hemisphere atmospheric circulation from 1000 to 2100 AD. *Climate Past*, **10**, 537–550, <https://doi.org/10.5194/cp-10-537-2014>.
- Schmidt, H., and H. von Storch, 1993: German Bight storms analysed. *Nature*, **365**, 791–791, <https://doi.org/10.1038/365791a0>.
- Schmith, T., 1995: Occurrence of severe winds in Denmark during the past 100 years. *Proc. Sixth Int. Meeting on Statistical Climatology*, Galway, Ireland, The Steering Committee for International Meetings on Statistical Climatology, 83–86.
- , H. Alexandersson, K. Iden, and H. Tuomenvirta, 1997: North Atlantic-European pressure observations 1868–1995 (WASA dataset version 1.0). Danish Meteorological Institute Tech. Rep. 97-3, 14 pp., https://www.dmi.dk/fileadmin/user_upload/Rapporter/TR/1997/tr97-3.pdf.
- , E. Kaas, and T. S. Li, 1998: Northeast Atlantic winter storminess 1875–1995 re-analysed. *Climate Dyn.*, **14**, 529–536, <https://doi.org/10.1007/s003820050239>.
- Trenberth, K. E., and Coauthors, 2007: Observations: Surface and atmospheric climate change. *Climate Change 2007: The Physical Science Basis*, S. Solomon et al., Eds., Cambridge University Press, 235–336.
- Ulbrich, U., and M. Christoph, 1999: A shift of the NAO and increasing storm track activity over Europe due to anthropogenic greenhouse gas forcing. *Climate Dyn.*, **15**, 551–559, <https://doi.org/10.1007/s003820050299>.
- Walker, A. M., 1968: A note on the asymptotic distribution of sample quantiles. *J. Roy. Stat. Soc.*, **30B**, 570–575.
- Wan, H., X. L. Wang, and V. R. Swail, 2010: Homogenization and trend analysis of Canadian near-surface wind speeds. *J. Climate*, **23**, 1209–1225, <https://doi.org/10.1175/2009JCLI3200.1>.
- Wang, X. L., F. W. Zwiers, V. R. Swail, and Y. Feng, 2009: Trends and variability of storminess in the northeast Atlantic region, 1874–2007. *Climate Dyn.*, **33**, 1179–1195, <https://doi.org/10.1007/s00382-008-0504-5>.
- , and Coauthors, 2011: Trends and low-frequency variability of storminess over western Europe, 1878–2007. *Climate Dyn.*, **37**, 2355–2371, <https://doi.org/10.1007/s00382-011-1107-0>.
- , Y. Feng, G. P. Compo, F. W. Zwiers, R. J. Allan, V. R. Swail, and P. D. Sardeshmukh, 2014: Is the storminess in the Twentieth Century Reanalysis really inconsistent with observations? A reply to the comment by Krueger et al. (2013b). *Climate Dyn.*, **42**, 1113–1125, <https://doi.org/10.1007/s00382-013-1828-3>.
- Wanner, H., S. Brönnimann, C. Casty, D. Gyalistras, J. Luterbacher, C. Schmutz, D. B. Stephenson, and E. Xoplaki, 2001: North Atlantic Oscillation—Concepts and studies. *Surv. Geophys.*, **22**, 321–381, <https://doi.org/10.1023/A:1014217317898>.
- WASA Group, 1998: Changing waves and storms in the northeast Atlantic? *Bull. Amer. Meteor. Soc.*, **79**, 741–760, [https://doi.org/10.1175/1520-0477\(1998\)079<0741:CWASIT>2.0.CO;2](https://doi.org/10.1175/1520-0477(1998)079<0741:CWASIT>2.0.CO;2).
- Weisse, R., and H. von Storch, 2009: *Marine Climate and Climate Change: Storms, Wind Waves and Storm Surges*. Springer Praxis, 219 pp.
- , and Coauthors, 2009: Regional meteorological–marine reanalyses and climate change projections: Results for northern Europe and potential for coastal and offshore applications. *Bull. Amer. Meteor. Soc.*, **90**, 849–860, <https://doi.org/10.1175/2008BAMS2713.1>.
- Zeileis, A., and G. Grothendieck, 2005: zoo: S3 infrastructure for regular and irregular time series. *J. Stat. Software*, **14**, 1–27, <https://doi.org/10.18637/jss.v014.i06>.